POLITECNICO DI TORINO
Repository ISTITUZIONALE

Boosting biocompatibility and minimizing inflammation in electrospun polyvinylidene fluoride (PVDF) cardiac patches through optimized low-pressure plasma treatment

Original
Boosting biocompatibility and minimizing inflammation in electrospun polyvinylidene fluoride (PVDF) cardiac patches through optimized low-pressure plasma treatment / Montalbano, G., Barberi, J., Benedetto Mas, A., Tung, T., Melo, P., Dalgarno, K., Silva, E.D., Gomes, R.N., Nascimento, D.S., Fiorilli, S., Vitale Brovarone, C.. - In: BIOMATERIALS ADVANCES. - ISSN 2772-9508. - 179:(2026). [10.1016/j.bioadv.2025.214488]

Availability:
This version is available at: 11583/3002915 since: 2025-09-10T12:21:32Z

Publisher:
Elsevier

Published
DOI:10.1016/j.bioadv.2025.214488

Terms of use:

This article is made available under terms and conditions as specified in the corresponding bibliographic description in the repository

Publisher copyright

(Article begins on next page)

26 June 2026

Biomaterials Advances 179 (2026) 214488

Contents lists available at ScienceDirect

Biomaterials Advances

journal homepage: www.journals.elsevier.com/materials-science-and-engineering-c

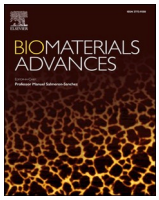

Boosting biocompatibility and minimizing inflammation in electrospun polyvinylidene fluoride (PVDF) cardiac patches through optimized low-pressure plasma treatment

G. Montalbano [a,*,1], J. Barberi [a,1], A. Benedetto Mas [a], T. Tung [b], P. Melo [b], K. Dalgarno [b], E.D. Silva [c,d,e], R.N. Gomes [c,d,e], D.S. Nascimento [c,d,e], S. Fiorilli [a,*], C. Vitale-Brovarone [a]

[a] Department of Applied Science and Technology (DISAT), Politecnico di Torino, Corso Duca Degli Abruzzi 24, 10129 Torino, Italy
[b] School of Mechanical and Systems Engineering, Newcastle University, Newcastle-upon-Tyne NE1 7RU, UK
[c] Institute for Research and Innovation in Health (i3S), University of Porto, Porto, Portugal
[d] Instituto Nacional de Engenharia Biomédica, University of Porto (INEB), Porto, Portugal
[e] Instituto de Ciências Biomédicas Abel Salazar, University of Porto (ICBAS), Porto, Portugal

ARTICLE INFO

Keywords:
PVDF
Electrospun patches
Plasma
Surface treatments
Hydrophilicity
Biocompatibility

ABSTRACT

Tailoring surface characteristics is key to guiding scaffold interaction with the biological environment, promoting successful biointegration while minimizing immune responses and inflammation.

In cardiac tissue engineering, polyvinylidene fluoride (PVDF) is a material of choice for its intrinsic piezoelectric properties, which can be enhanced through electrospinning, also enabling the fabrication of nanofibrous structures mimicking native tissue. However, the inherent hydrophobicity of PVDF can hinder its integration with biological tissues.

To overcome this limitation, electrospun PVDF patches were subjected to radio-frequency low-pressure O_2 plasma treatment to enhance surface hydrophilicity and overall biocompatibility. A systematic experimental study identified optimal parameters, revealing that higher gas content and prolonged exposure are preferable to high power levels, which deteriorate the patch's morphological and mechanical properties.

X-ray photoelectron spectroscopy confirmed the formation of oxygen-containing surface groups, resulting in the patch's superhydrophilicity. Preservation of the fibrous nanostructure and electroactive phase content was verified using scanning electron microscopy and infrared spectroscopy combined with differential scanning calorimetry, respectively. The optimized plasma treatment maintained the patch's elasticity and demonstrated long-term stability for up to 3 months.

In vitro biocompatibility was assessed through indirect and direct tests using AC16 human cardiomyocytes and neonatal human dermal fibroblasts, revealing good cell viability, adhesion, and spreading over 7-days. Finally, plasma-treated patches demonstrated strong adhesion to the myocardial tissue and exhibited markedly reduced inflammatory response compared to the untreated controls, as shown by decreased $CD45^+$ immune cell infiltration around the patch implanted in infarcted mice, highlighting the surface treatment's effectiveness in enhancing *in vivo* biocompatibility.

1. Introduction

The interaction between biomaterials and the biological environment is crucial for the success of scaffolds and implanted medical devices, and to this aim, engineered interfaces can significantly improve clinical outcomes. Tailoring the surface properties of biomaterials and implants is thus essential for achieving optimal biointegration and minimizing adverse reactions, such as excessive immune and inflammatory response [1–3].

Besides surface properties, successful biointegration and functional regeneration are also critically dependent on the ability of biomaterials to match the mechanical and biological characteristics of the host tissue,

* Corresponding authors.
E-mail addresses: giorgia.montalbano@polito.it (G. Montalbano), sonia.fiorilli@polito.it (S. Fiorilli).
[1] Equal contribution.

https://doi.org/10.1016/j.bioadv.2025.214488
Received 27 June 2025; Received in revised form 29 August 2025; Accepted 1 September 2025
Available online 2 September 2025
2772-9508/© 2025 The Authors. Published by Elsevier B.V. This is an open access article under the CC BY license (http://creativecommons.org/licenses/by/4.0/).

aiming to closely mimic its native features. Accordingly, in the specific context of cardiac tissue engineering, particular attention is devoted to the design of constructs capable of supporting and promoting electromechanical coupling with the heart. Given the adverse immune responses often triggered by allogenic and xenogeneic scaffolds, polymeric piezoelectric materials are emerging as a promising and viable alternative [4,5].

Polyvinylidene fluoride (PVDF) is widely reported in the literature, as non-degradable thermoplastic fluoropolymer, recognised for its piezoelectric properties and already approved by the Food and Drug Administration (FDA) for use in various commercially available clinical devices [6].

Piezoelectric polymers are classified as smart biomaterials that respond to mechanical stress by inducing transient surface charge variations, which in turn lead to changes in the electrical potential within the material, without requiring additional energy sources or wired electrodes. The piezoelectricity of PVDF and its copolymers (*e.g.*, PVDF-HFP, PVDF-TrFE) is strictly related to the content of electroactive β-phase, which can be increased by the synergistic effect and simultaneous application of both mechanical stretching and electrical poling during the electrospinning manufacturing process, directly causing dipoles alignment [4]. Electrospinning of PVDF-based materials can thus lead to the production of flexible, lightweight fibrous sheets that can serve both as 3D scaffolds and sensors, where the electrical signal is downscaled at the cellular level thanks to the presence of ultrafine nanometric fibres [7]. The unique properties of PVDF-based piezoelectric materials make them particularly advantageous for cardiac applications, as they harness the continuous wall deformation caused by cardiac contractions to enhance electrical conduction, especially when it is impaired, as in the case of myocardial infarction (MI) [8]. However, despite the advantages of using PVDF, its inherent highly hydrophobic nature may compromise the surface biocompatibility and, consequently, the overall performance of the construct [9], resulting in sustained inflammatory infiltration in the patch surrounding tissue. Different surface modification techniques, such as chemical grafting, physical vapor deposition, defluorination-sulfonation, O_3/O_2 reactivation, blending, and electron beam radiation have been proven to efficiently increase the hydrophilicity of PVDF-based devices [10]. However, each of these methods has exhibited various limitations, primarily related to high costs, long processing times, complexity and alterations of the bulk properties of the materials [9].

In this scenario, plasma treatments have emerged as a versatile, fast and effective approach for surface modification for both porous and non-porous polymeric materials, while potentially preserving the bulk properties of the construct upon adequate process optimization.

Plasma treatment leverages the action of ionized gases to activate surfaces and induce chemical modification to a different extent, including the generation of surface reactive species and the introduction of functional groups, up to the creation of specific coatings [11]. Various gases and their combination can be exploited to achieve specific modifications on PVDF surfaces: O_2 plasma was reported to significantly enhance cell adhesion and density, H_2 proved highly effective for surface defluorination, while Ar was associated with a significant enhancement of surface roughening and free radical polymerization [9,12].

Although plasma treatments on PVDF-based materials have been previously explored, most studies lack thorough optimization of treatment parameters for long-term stability and do not fully evaluate the final properties of the constructs. The high energy involved during the treatment can in fact potentially lead to morphological and mechanical alterations, while surface chemical modifications may result in a reduction of the electroactive phase, thereby impairing the final piezoelectric properties [12,13]. Moreover, besides the considerable variability in available data, biological evaluation of plasma-treated PVDF constructs in the specific context of cardiac tissue engineering is mostly limited to the assessment of non-human cardiomyocyte adhesion driven by enhanced surface wettability [3].

Here, we explore optimization of PVDF processing by electrospinning for a specific cardiac application: a patch designed for epicardial placement following MI, with the long-term goal of locally supporting tissue remodeling. Preserving the piezoelectric properties and ensuring the absence of adverse reactions upon implantation are therefore critical to achieving this challenging objective.

Accordingly, the present study seeks to optimize and confirm the efficacy of radio-frequency (RF) low-pressure O_2 plasma (LPP) treatments in enhancing the surface hydrophilicity of electrospun PVDF patches, ultimately improving their biocompatibility *in vitro* and *in vivo*.

To address existing gaps in the literature, the LPP treatment was systematically optimized through a comprehensive evaluation of key parameters, including gas flow rate, power, exposure time, and the use of Ar as a stabilizing gas, with the objective of enhancing surface hydrophilicity, while preserving the patch's structural and functional properties.

After establishing the optimal set of parameters, the resulting patches were thoroughly characterized for their nanostructure, crystalline phase content, and mechanical properties using scanning electron microscopy, infrared spectroscopy, and tensile testing, respectively. X-ray photoelectron spectroscopy was employed to confirm successful surface modification, and the stability of the optimized treatment was further evaluated over a period of up to three months.

Based on the cellular composition of myocardial tissue, the *in vitro* cytocompatibility of the developed patches was confirmed through the adhesion and proliferation of AC16 human cardiomyocytes and Neonatal Human Dermal Fibroblasts (NHDF), as assessed by both direct and indirect assays. This has shown that improved hydrophilicity allows for better cell attachment, which in turn means that the patch is better tolerated on implantation.

Finally, the ability of the plasma-treated patches to reduce the inflammatory response was successfully evaluated *in vivo*, following the induction of myocardial infarction in a murine model.

Considering previous reports of plasma treatments of PVDF for tissue regeneration, the present work represents a step forward. Through thorough process optimization and precise adjustment of power and exposure time, enhanced hydrophilicity was achieved [1] while preserving key scaffold properties, including fiber topography [14]. We also addressed potential limitations associated with the use of animal cells [3] and introduced a reliable quantitative method for evaluating the immunomodulatory effects of plasma-treated patches.

2. Materials and methods

2.1. Design of PVDF patches by electrospinning

Based on previous protocol reported in the literature [7,15], PVDF powders (Sigma-Aldrich®, Mw: 180.000 g/mol) were dissolved in a mixture of 50:50 acetone (Honeywell, Riedel-de Haën™) and DMSO (Uvasol®, Merck KGaA) to reach a final concentration of 18 wt%.

The resulting solution was subsequently processed by a LE-50 Fluidnatek electrospinning system (Bioinicia, Spain) equipped with a 10 cm diameter rotating collector at 2000 rpm to promote fiber alignment. The electrospinning process was conducted by setting a distance between the spinneret tip and collector of 12 cm (working distance) with a voltage and flow rate of 20 kV and 1.4 mL/h, respectively, to obtain a stable material jet. The electrospinning was carried out for 3 h to obtain a final PVDF patch thickness of about 150 ± 20 μm.

2.2. Plasma treatments on electrospun PVDF patches

A low-pressure plasma instrument Femto (Diener electronic GmbH & Co. KG, Germany) equipped with a 13.56 MHz radio frequency plasma generator was used for surface modification. The plasma treatment was optimized upon assessment of different sets of parameters, as well as the combination of O_2 and Ar gas flows. In detail, different treatments were

explored by varying plasma power between 45 and 300 W, working pressure between 0.1 and 0.5 mbar, and exposure times between 30 and 180 s. Gas flow rates were determined according to the pressure set in the plasma chamber.

2.3. Characterisation of PVDF patches before and after plasma treatment

2.3.1. Water contact angle measurements

The water contact angle was measured using a Drop Shape Analyzer DSA100S (KRÜSS, Germany). The analysis was performed by depositing a 10 μL drop of distilled water on the sample surface, and the measure was taken after 15 s upon drop deposition. Data were obtained by averaging over three measurements in different areas on the sample's surface.

2.3.2. Morphological assessment

For investigation of fiber morphology and diameter before and after plasma treatment, PVDF patches were punched into 10–12 mm disks, platinum coated using a Q150T S Sputter Coater (Quorum Technologies, U.K.) and then imaged using a scanning electron microscope Phenom XL (Phenom-World B.V., The Netherlands) with an accelerating voltage of 10 kV. The collected images were further processed by ImageJ software to define more precisely the resulting distribution and mean value of fiber diameters. A greater detail of the PVDF fiber surface was obtained through Field-Emission Scanning Electron Microscopy (FESEM) using a Zeiss Merlin instrument.

2.3.3. Physico-chemical characterisation

X-ray Photoelectron Spectroscopy (XPS) was used to detect changes in surface chemistry due to the plasma treatment. The spectra were obtained using a PHI 5000 Versa Probe (Physical Electronics, Germany) photoelectron spectrometer and a Kα line with an energy of 1486.6 eV and a take-off angle of 45°. The samples' composition was calculated from survey spectra, while the chemical groups were obtained by high-resolution spectra collected in the regions of C1s and O1s. Deconvolution was performed with the software CasaXPS (Casa Software Ltd., U.K.) using a Gaussian-Lorentzian 70–30 peak shape and a Shirley background. Before deconvolution, the spectra were calibrated against the CF_2 peaks at 291.4 eV [16].

Infrared measurements (FTIR) were performed at room temperature using a FTIR Tensor 27 Spectrometer (Bruker Optics) in the Attenuated Total Reflection (ATR) mode from 4000 to 600 cm^{-1}. FTIR spectra were collected after 64 scans with a resolution of 2 cm^{-1}. The spectra collected were further used to quantify the relative amount of α, β and γ phases (F_α, F_β, F_γ, respectively) of PVDF using the following Equations:

$$F_{EA}\ (\%) = \left[I_{EA} \Big/ \left(\left(k_{840}/k_{763}\right) I_{763} + I_{EA} \right) \right] \times 100 \quad (1)$$

$$F_a\ (\%) = 100 - F_{EA} \quad (2)$$

$$F_\beta\ (\%) = F_{EA} \left[\Delta h_{\beta'} \Big/ \left(\Delta h_{\beta'} + \Delta h_{\gamma'} \right) \right] \text{x} 100 \quad (3)$$

$$F_\gamma\ (\%) = F_{EA} - F_\beta \quad (4)$$

where F_{EA} represents the electroactive phases β and γ; I_{EA} and I_{763} are the absorbance at 840 and 763 cm^{-1}; k_{840} and k_{763} are the absorbance coefficients at 840 and 763 cm^{-1}, *i.e.* 7.7×10^4 and 6.1×10^4 cm^2 mol^{-1}; $\Delta h_{\beta'}$ is the difference between the peak at 1275 cm^{-1} and the valley at 1260 cm^{-1}, and $\Delta h_{\gamma'}$ is the difference between the peak at 1234 cm^{-1} and the valley at 1225 cm^{-1}.

Differential Scanning Calorimetry measurements (DSC) were performed in a Mettler Toledo DSC apparatus (Milan, Italy) from 30 to 200 °C, with a heating rate of 10 °C/min and under nitrogen purge. ATR-FTIR and DSC analyses were combined to determine the crystalline content of PVDF before and after plasma treatment, according to Eq. S1 reported in the Supplementary Information.

The piezoelectric coefficient d_{33} was determined using a piezoelectric evaluation system (TFAnalyzer 2000HS, Aixacct, Aachen, Germany) in conjunction with a single-point laser vibrometer (OVDF-505, Polytec, Inc., Irvine, USA). Piezoelectric hysteresis loops were obtained by applying an alternating voltage in the frequency range of 1–10 kHz and recording the resulting displacement along the same direction, perpendicular to the patches. The d_{33} values were extracted by interpolating the linear portion of the displacement-voltage curves. Prior to measurement, circular platinum electrodes (2 mm diameter) were deposited on the sample surfaces *via* sputter coating. The piezoelectric coefficients of PVDF fibres before and after the plasma treatment were evaluated.

2.3.4. Tensile tests

PVDF patches were tensile tested according to the ISO 527-5 A standard (using a dog-bone test specimen) to assess their elastic modulus, strength and elongation at break. An INSTRON 5966 Mechanical Testing System was used, equipped with a 50 N load cell and compressed air clamps. Tensile tests were performed on 5 samples whose thickness was measured before analysis. All specimens were preloaded with 0.1 N to remove any misalignment effects and then pulled at a constant speed of 10 mm/min until reaching sample failure.

The stress was calculated as the ratio between the load and the cross-section area of a tensile specimen, while the strain was calculated as the ratio between its extension and its initial length. The Young's modulus value was extracted from the stress/strain curve.

2.3.5. Long-term stability of the optimized plasma treatment

Once the optimal plasma treatment was established, the stability of the surface modification was assessed over a period of up to three months, with patches stored in sealed plastic bags. At predefined time points, samples were retrieved and analyzed using contact angle measurements, SEM, and ATR-FTIR, and the results were compared to those obtained immediately after treatment.

2.4. In vitro biological assessment

2.4.1. Materials

Heat Inactivated Fetal Bovine Serum (FBS), 4 % (*v*/v) Paraformaldehyde (PFA) in Phosphate Buffer Solution (PBS) and Trypsin-EDTA (0.25 %) were purchased from Fisher Scientific (U.K.), Dulbecco Modified Eagle Medium/Nutrient Mixture F12 with L-glutamine (DMEM/F12, D8437) and Dulbecco Modified Phosphate Buffer Saline (DPBS) were purchased from Sigma Aldrich (U.K.) and O-rings (FKM, 6 mm Bore, 12 mm Outer diameter, 196–5806) from RS components (U.K.).

2.4.2. Cell culture for direct and indirect assays

AC16 cardiomyocytes (Millipore. U.K.) at passage 8 and Neonatal Human Dermal Fibroblasts (Neo-NHDF, Lonza, U.K.) at passage 12 were cultured with DMEM/F12 basal medium supplemented with 10 % FBS, 100 μg/mL of Penicillin/Streptomycin, incubated at 37 °C in an atmosphere of 5 % CO_2. Cells were washed with DPBS, followed by detachment using 0.25 % Trypsin-EDTA, centrifuged at 400 x*g* and resuspended in DMEM/F12 for seeding.

For the direct contact assay, the patches were cut using a surgical scalpel into squares measuring approximately 13 × 13 mm and placed into 48-well plates. Samples were secured to the bottom with an O-ring, previously sterilised. Prior to cell seeding, the patches placed in the 48-well plate were conditioned with complete DMEM/F12 medium and incubated at 37 °C for 1 h before cell seeding. The conditioning medium was removed from the well, and cells were seeded at a density of 20,000 cells/well and topped up with DMEM/F12 medium again. Cells seeded onto the tissue culture plastic (TCP), with and without an O-ring, were used as controls.

For the indirect assay, one day prior to the start of the experiment, the patches were immersed in complete DMEM/F12 medium, at a ratio

of 1 mg/mL (material/media), and incubated at 37 °C overnight, thus creating the conditioned medium. On the second day, the cells were seeded into 48-well plates, at a density of 20,000 cells/well, and cultured with the conditioned media for 7 days. Cells exposed to unconditioned media were used as a control.

For both direct and indirect assays, samples were analyzed after 1, 3 and 7 days of culture.

To perform the *in vitro* biological assessment, PVDF patches and PVDF patches subjected to the optimized plasma treatment (P_PVDF) were sterilised under UV light, and O-rings were autoclaved for 30 min prior to testing.

2.4.3. Cell viability and proliferation

Cell viability was assessed *via* Live/Dead Viability/Cytotoxicity kit (Invitrogen, U.K.). The Live/Dead working solution was added to the cells after the removal of media and washing with DPBS. Samples were incubated for 40 min at room temperature, protected from light, and subsequently washed with PBS. Images were obtained with the fluorescence microscope EVOS M5000 (Invitrogen, U.K.).

Quant-iT PicoGreen dsDNA assay kit (Invitrogen, UK) was used to determine the amount of DNA available in each sample, enabling the estimation of cell proliferation. Briefly, media was aspirated from each well and samples were stored at −80 °C until the end of the culture period. To lyse the cells and access their DNA, samples were thawed and immersed in a solution of 0.1 % Triton X-100 (Sigma Aldrich, UK) in DNase/RNase free water (Invitrogen, UK), then incubated at 37 °C for 1 h. Subsequently, the Quant-iT PicoGreen dsDNA assay was used, and the fluorescent intensity was measured in the FLUOstar Omega microplate reader (BMG Labtech), applying an excitation filter at 485 nm and an emission filter at 520 nm. Results were compared against a previously prepared standard curve.

2.4.4. Immunofluorescence analysis

Samples were fixed with 4 % (*v*/v) PFA at room temperature for 30 min and washed with DPBS three times for 5 min at room temperature. The samples were then permeabilized using 0.1 % Triton X-100 in DPBS at room temperature for 1 h, followed by three DPBS washes for 5 min each at room temperature. The actin staining was prepared by mixing 1 drop of ActinRed 555 (ReadyProbes, Invitrogen, U.K.) per 1 mL of DPBS. The working solution was added to the samples, which were incubated for 30 min at room temperature and protected from light. The nucleus was stained using DAPI (Thermo Scientific, U.K.) dissolved in DPBS at a ratio of 1:1000. After three washes with DBPS, samples were incubated in this solution at room temperature for 15 min, protected from light. Fluorescent images were acquired using an EVOS M5000 fluorescent microscope.

2.4.5. Statistical analysis

Tests were performed on triplicates of each sample, and results were presented as mean value ± standard deviation. Unpaired Student's *t*-test or two-way ANOVA with Tukey's multiple comparisons test were performed with GraphPad Prism 10 software (GraphPad, USA) using a level of significance of $p < 0.05$ (*), $p < 0.01$ (**), $p < 0.001$(***) and $p < 0.0001$ (****).

2.5. In vivo biological assessment

2.5.1. Myocardial infarction model

The mice experiments were performed at i3S (Instituto de Investigação e Inovação em Saúde) (Porto, Portugal). All experimental protocols were authorized by the internal Institutional Animal Care and Use Committee (IACUC) and the national veterinary agency. *In vivo* experiments were conducted using a user-blinded approach to minimize bias in data collection and analysis. Eight-week-old C57BL/6 mice (Charles River) were subjected to myocardial infarction (MI) by permanent ligation of the left anterior descending (LAD) coronary artery as described in [17]. At the time of MI induction, PVDF and P_PVDF patches were cut with a sterile 4 mm round puncher and attached to the epicardial surface of the heart, below the ligation site, using 10 μL of fibrin glue (F3879, Merck). Analgesia was provided by adding paracetamol (30 mg/mL) in drinking water and buprenorphine intraperitoneal injections every 12 h for 3 days or until complete recovery. Hydration was reinforced with subcutaneous injections of glucose (5 %) saline (B. Braun) every 12 h.

2.5.2. Heart collection and histology

Animals were weighed and sacrificed 14 days after MI. The mice were induced with 4 % isoflurane and, after verifying unresponsiveness, asystole was induced by intracardiac injection of 4 M potassium chloride, followed by heart collection. After dissection of the main vessels, the hearts were weighted, and images were acquired in a stereomicroscope (Olympus). The hearts were then fixed in formalin for 16 h at 4 °C. Following fixation, the hearts were processed, embedded in paraffin, and transversely sectioned. Serial 3 μm sections were obtained at 270 μm intervals as detailed in a previous study in the literature [18].

Sections were either stained using Masson's Trichrome staining according to the manufacturer's protocol (HT15, Sigma Aldrich) or prepared for immunostaining. For immunostaining, sections were deparaffinized, washed, permeabilized with 0.2 % Triton X-100, and blocked for 1 h at room temperature with a blocking buffer containing 1 % bovine serum albumin and 4 % fetal bovine serum in PBS. Primary antibodies against α-sarcomeric actin (A129, Sigma, 1:400) and CD45 (AF114, R&D, 1:200) were incubated overnight at 4 °C in blocking buffer. The following day, sections were washed and incubated for 1 h with secondary antibodies donkey anti-mouse IgM 488 (715–545-140, Jackson Labs, 1:1000) and donkey anti-goat IgG 647 (A21447, Invitrogen, 1:1000) in blocking buffer. Finally, the sections were counterstained with DAPI and mounted in VECTASHIELD Antifade Mounting Medium (Vector Laboratories).

2.5.3. Imaging and automatic quantification of CD45-positive cells

Immunofluorescence images were acquired using a high-throughput Operetta CLS microscope (Revvity) with a 40× water objective. Imaging was performed in the left ventricle wall region where the patches was implanted. Automatic detection of CD45-positive cells was carried out using the built-in Harmony Software.

The patch area was identified by exploiting its autofluorescence in the green channel. The cell area surrounding the patch was user-defined based on a general intensity threshold. Nuclei were detected in the DAPI channel, and a ring around each nucleus was created to establish a region for detecting the CD45 fluorescence signal. CD45-positive cells were identified within this surrounding patch area using a defined-intensity threshold.

2.5.4. Statistical analysis

Statistical testing was performed using GraphPad® Prism 8.0 Software. Outliers were excluded by ROUT analysis (Q = 1 %). Shapiro-Wilk test was used to evaluate normal distribution of data. Normally distributed data were tested with independent sample Student's *t*-test.

3. Results and discussion

3.1. Design and characterisation of PVDF electrospun patches

The use of polyvinylidene fluoride (PVDF) as a constituent material in the design of electroactive patches and devices for cardiac tissue engineering appears particularly promising, especially when combined with electrospinning technologies. This approach takes advantage of the opportunity to enhance the material's piezoelectric properties while producing flexible, nanofibrous membranes that can function both as 3D scaffolds and sensors [4].

In this study, based on previous data in the literature [7,19], a

piezoelectric nanofibrous patch was obtained by processing a 18 wt% PVDF solution in 50:50 Acetone:DMSO solvent with a commercial Fluidnatek LE-50 electrospinning machine (Bioinicia, Spain), where a rotating collector was exploited to promote the alignment of the fibres in an attempt to mimic the anisotropic feature of the native cardiac tissue. Moreover, unlike more conventional solvents such as dimethylformamide (DMF) and chloroform [1,4], the feeding polymeric solution was optimized using a mixture of acetone and DMSO, aiming to reduce the environmental and safety impact of the process and further improve the biocompatibility of the resulting patches.

As shown in Fig. 1A, the electrospinning process led to the successful formation of PVDF patches featuring a homogeneous fibrous network with aligned fibres characterized by a constant diameter along their axis of 280 ± 10 nm, as confirmed by scanning electron microscopy (SEM) images.

Due to the good stability of the polymer jet following the optimization of different parameters, the electrospinning process was carried out for 3 h to reach a thickness of approximately 150 μm, ensuring adequate handling of patches even during the biological assessment and *in vivo* implantation.

The physico-chemical characterisation of PVDF patches by attenuated total reflection Fourier-transform infrared spectroscopy (ATR-FTIR) enabled the detection of the different crystalline phases of the polymer, thanks to the vibrational mode characteristic of each phase, *i.e.*, α, β, and γ. According with data in the literature, the typical FTIR spectrum for electrospun PVDF shows the band at 763 cm^{-1} related to the α phase, while the electroactive γ and β phases give a contribute at 840 cm^{-1}, 1234 cm^{-1} and 1275 cm^{-1} (Fig. 1B), with the piezoelectric β phase counting for about 94.7 ± 1.0 % of the crystalline content [19–21].

The overall crystallinity was evaluated by firstly defining the phase composition by ATR-FTIR followed by Differential Scanning Calorimetry (DSC) measurements (Fig. S1, Supplementary Information) and calculating a final value of 48 ± 5 % [9].

Overall, the high crystallinity of the resulting material, and particularly the predominance of the piezoelectric β phase, can be attributed to the synergistic effect of the elevated voltage and the high rotational speed of the drum collector during the electrospinning process. This combination induces pronounced stretching of the polymer jet and promotes molecular alignment, ultimately facilitating the formation of the β phase [6].

As expected by the crystalline structure and the ß phase presence, the fibres exhibited a piezoelectric behaviour, being able to deform under application of an oscillating high voltage. The obtained d_{33} coefficient is equal to −6.3 ± 0.6 pm/V, a value in accordance with the existing literature [6,22], which has been reported to be suitable to support CMs activity [23]. Moreover, as evident in Fig. 1C and supported by the literature, the pronounced hydrophobic nature of PVDF was confirmed through water contact angle θ (WCA) measurements, yielding a mean WCA value of 116 ± 4°.

3.2. Optimisation of the low-pressure plasma (LPP) treatment

Highly hydrophobic surfaces are generally unfavorable for biomaterials and devices designed for cellular contact and implantation, as they may trigger excessive inflammatory responses and ultimately impair biointegration. Plasma-based surface activation has demonstrated effectiveness in enhancing polymer wettability by selectively modifying surface chemistry and potentially introducing polar functional groups. [16]. In this context, low-pressure plasma (LPP) offers a promising, fast and effective strategy for modifying PVDF surfaces, in which Ar and O_2, used individually or in combination, are commonly employed as working gases in this process [24]. Despite their prior use, there is limited clear evidence in the literature regarding the impact of different parameters and gases not only on surface properties, but also on the bulk characteristics of materials and their long-term stability [24].

In the specific case of PVDF-based substrates, the use of O_2 and Ar plasma, as reactive and stabilizing gases respectively, was reported to be effective and versatile for achieving highly hydrophilic surfaces. However, recent studies often present conflicting results and incomplete characterizations. Accordingly, while Ar alone is not typically associated with a significant reduction in WCA, the study conducted by Duca and colleagues [13] demonstrated a marked increase in the surface wettability of PVDF following exposure to Ar plasma.

Moreover, as an additional variable in the process, the production method of the patch and its morphological features may also impact the plasma treatment efficacy [10,24,25]. In fact, Park et al. [26] reported that O_2 plasma was ineffective in reducing the WCA of PVDF sheet surfaces.

Based on this, a systematic study was then carried out with the aim of efficiently and stably reducing the hydrophobic properties of the developed electrospun PVDF patches by using a low-pressure 13.56 MHz plasma machine and exploring different parameters over a wide range of values and combinations. In accordance with the various conditions reported in the literature and the parameters permitted by the equipment, the working atmosphere composition (O_2%; Ar%), the exposure time, the plasma power and the pressure were varied in the range reported in Table 1.

As a preliminary indication of the plasma treatment's efficacy, the surface water contact angle (WCA) was measured on the patches obtained from an extensive set of experiments where the different process

Table 1
Ranges of the parameters varied during the optimisation of the LPP treatment.

Process parameter	Range
Time	30–180 s
Power	45–300 W
Atmosphere	0–100 % O_2 in Ar
Pressure	0.1–0.5 mbar

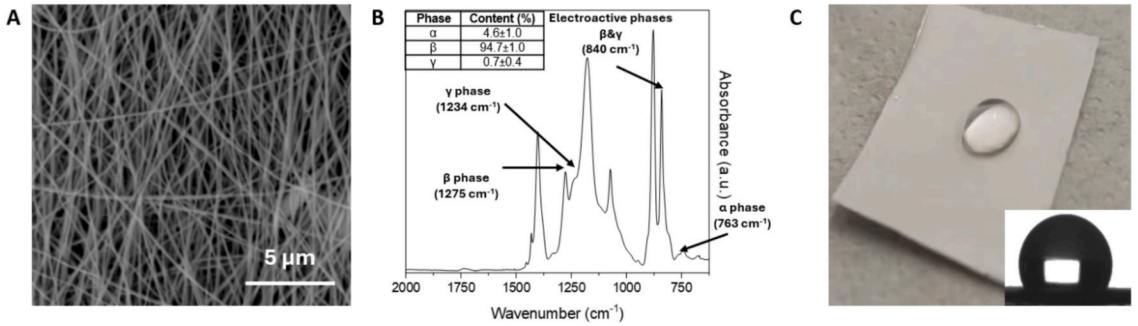

Fig. 1. SEM image showing the aligned nanofibrous structure (A), ATR-FTIR spectrum (B), surface hydrophobicity and water contact angle (C) of PVDF patches.

parameters were varied within the entire selected range, as detailed in Table S1 (Supplementary Information).

This initial assessment enabled the identification of a set of parameters capable of significantly altering surface properties, resulting in a highly hydrophilic character. In such cases, the combination of improved hydrophilicity and the high porosity of the electrospun patch led to rapid droplet spreading and adsorption due to capillary effects [27], preventing an accurate measurement of the contact angle. The contact angle due to the chemical modification of the PVDF was hypothesized to be below 40°, in agreement with previous literature reports [16,28]. The combination of plasma treatment and the porous structure resulted in a superhydrophilic-like behaviour of the P_PVDF patches.

As a first finding, the study revealed that high O_2 content and increased chamber pressures (0.5 mbar) are the key parameters for achieving an effective reduction in the WCA. Conversely, low or negligible O_2 levels, as well as low gas pressures (0.1 mbar), were found to be ineffective in modifying the patch surface, resulting in WCA values higher than 90°. These results confirmed the need for a higher density of reactive species, given by the presence of O_2, to induce a significant modification of surface chemistry. Accordingly, the efficacy of the treatment on PVDF substrates is associated with the cleavage of C—F and C—O bonds following plasma generation, and the subsequent introduction of surface polar COOH groups in the presence of oxygen [12].

In the presence of high O_2 concentrations, higher power levels and longer processing times are also consistently associated with a significant decrease in WCA. However, the high energy input and the potential subsequent increase in temperature induced changes in the morphological and mechanical properties of the patch as assessed on plasma-treated patches. Indeed, as visible in Fig. S2 (Supplementary Information), the combination of high powers (300 W) and long exposures (180 s) appreciably altered PVDF fiber morphology resulting in deformed or fused fibres. Moreover, despite retaining morphological features, the use of an intermediate power level (186 W) caused a significant decrease in the mechanical properties of the PVDF patches. This resulted in the samples becoming very brittle and impossible to manipulate, likely due to potential oxygen-induced surface erosion effects [13].

Based on this evidence, lower power setting (45 W) during the process is therefore preferable to avoid altering the overall material properties, while high O_2 concentrations (100 % O_2; 0.5 mbar) in combination with long plasma exposure time (180 s) finally proved to be effective and reproducible in achieving the surface superhydrophilicity of the PVDF patch.

3.3. Characterisation of the plasma treated PVDF (P_PVDF) patches

The electrospun PVDF patches, subjected to the optimized plasma treatment (100 % O_2, 45 W, 180 s, 0.5 mbar) and referred to as P_PVDF patches, were thoroughly characterized to facilitate a more detailed comparison with untreated PVDF patches and to confirm the preservation of their intrinsic properties.

As shown in Fig. 2, the preservation of the crystalline phase content and the resulting effective surface chemical modification of the P_PVDF patches were evaluated using ATR-FTIR and XPS analyses, respectively.

A comparison of the ATR-FTIR spectra from the analysis of PVDF and P_PVDF patches (Fig. 2A) confirms that the optimized plasma treatment did not cause any significant alterations in overall crystallinity or phase composition. Specifically, the two spectra exhibit no notable differences in the characteristic peaks or shifts, with the electroactive β phase remaining predominant, thereby confirming the preservation of the patch's piezoelectric phase. Accordingly, P_PVDF samples showed piezoelectric activity, with a measured d_{33} coefficient of 10.4 ± 5.2 pm/V, similar to those of untreated PVDF fibres.

The survey and high-resolution spectra taken in the C1s and O1s regions obtained from XPS, along with the subsequent peak deconvolution and fitting, enabled a precise analysis of the surface chemistry and the differences in the functional groups exposed after plasma treatment.

According to the chemical composition (Table S2, Supplementary Information) of PVDF (CH_2–CF_2), carbon (C) and fluorine (F) were detected in equal proportions, with a slightly higher carbon content indicating unavoidable carbonaceous contamination. Specifically, the carbon peaks of both PVDF and P_PVDF samples were primarily attributed to CH_2 and CF_2 groups in the main backbone, observed at binding energies of 286.9 eV and 291.4 eV, respectively [16]. Additionally, a peak at 288.8 eV in PVDF suggested the presence of carbonaceous contamination.

Conversely, as evidenced in Table S2 and Fig. 2B, P_PVDF samples

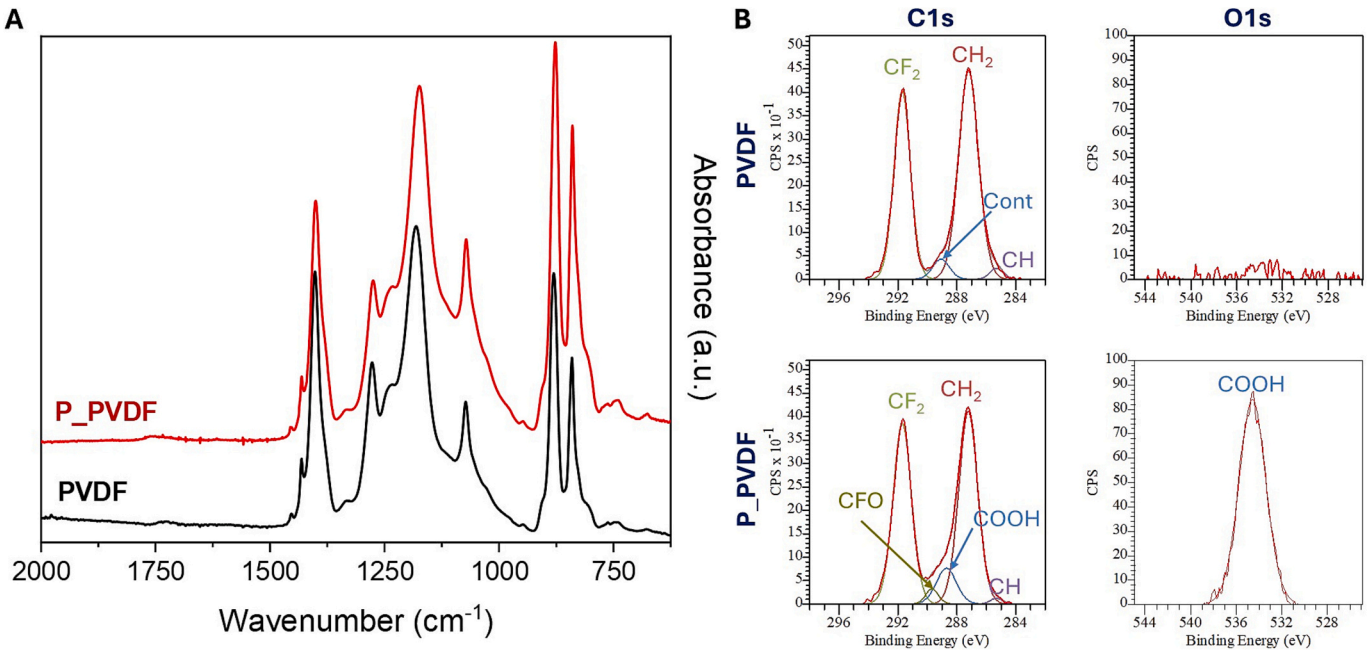

Fig. 2. ATR-FTIR (A) and XPS analysis (B) comparing PVDF and P_PDVF patches.

exhibited a reduction in fluorine (F) content in favor of oxygen (O), confirming the formation of oxygen-containing groups on the fiber surface during plasma treatment. In this process, fluorine atoms are removed and replaced by polar groups during exposure to O_2 [12,27]. Accordingly, the two peaks at intermediate energies, *i.e.* 288.4 eV and 289.4 eV, are attributed to COOH and CFO groups, while the peak at 534.6 eV in the O1s region corresponds to the formation of COOH groups [28]. This confirmed the successful incorporation of oxygenated moieties, which are responsible for the significant decrease in the surface hydrophobicity of the polymeric substrate.

After evaluating the effective surface modification and the overall preservation of the material's crystalline content, high-resolution morphological analysis and tensile mechanical tests were conducted to assess the retention of the patches' intrinsic properties.

FESEM images of the patch surface before (Fig. 3A, C) and after (Fig. 3B, D) plasma treatment revealed no differences in fiber diameter, morphology, or orientation, nor any variations in the nanoscale topography of electrospun PVDF fibres. This confirmed that lower-energy treatments are preferable for preserving the patch's nanostructure.

Preserving the structural characteristics also ensured the retention of the patch's good elasticity, as confirmed by mechanical tensile tests conducted in accordance with the ISO 527-5 A standard and shown in Fig. 3E.

The stress-strain deformation curves of PVDF and P_PVDF patches exhibited a similar trend, showing elastic deformation up to approximately 6 % elongation before reaching final failure at a deformation exceeding 50 %. The Young's modulus (E) was determined to be 65 ± 12 MPa, while the ultimate strength (σ_f) ranged between 10 and 20 MPa. Considerably, comparable mechanical properties were also reported for commercial patches already used in cardiac clinical applications, such as Dacron® and Gore-Tex®, further supporting the potential use of the developed patches in the specific field of interest [29].

Finally, the stability of the optimized plasma treatment was evaluated by storing the patches in sealed plastic bags for up to three months. Despite being kept in an uncontrolled environment, the P_PVDF patches maintained excellent wettability while preserving their morphological and physicochemical properties, as shown in Fig. S3 (Supplementary Information).

3.4. *In vitro cytocompatibility of PVDF and P_PVDF patches*

The functional interaction between cells and surfaces, along with the successful biointegration of patches and devices, is primarily influenced by various surface characteristics, followed by an adequate compliance with the regenerating host tissue. While hydrophilicity certainly plays a key role, a significant reduction in the water contact angle (WCA) following plasma treatment does not always correlate with enhanced biocompatibility of the entire system [3,30]. Accordingly, a comprehensive *in vitro* biological assessment using cardiac-specific cells was conducted to validate the overall biocompatibility of the developed patches, with particular emphasis on the system's enhanced performance following optimized plasma treatment.

The cytocompatibility of PVDF and P_PVDF patches was assessed using two approaches: (i) a direct evaluation to examine the effects of the patch in direct contact with cells, and (ii) an indirect analysis to investigate the potential impact of released substances. The tests performed encompassed cell viability, proliferation and morphology, focusing on cardiomyocytes and fibroblasts, as main components of myocardial tissue.

The results of the indirect assay were consistent across all tested sample groups and controls for both cell types. AC16 cardiomyocyte viability was confirmed from day 1 and maintained through day 7 (Fig. 4A), exhibiting a spindle-shaped morphology characteristic of these cells (Fig. 4C). Cells proliferated in all samples over the 7-day period, with good viability but a slower proliferation rate on P_PVDF patches compared to PVDF (Fig. 4E). Neo-NHDF cells also remained generally viable throughout the study (Fig. 4B), displaying their typical elongated, spread-out morphology (Fig. 4D). Cell proliferation occurred across all samples over the 7 days, with no significant differences between groups up to day 3. By day 7, P_PVDF samples showed lower DNA levels compared to PVDF (Fig. 4F), but neither material shows any cytotoxic behaviour, indicating that the materials do not leach or release any cytotoxic byproducts that could harm surrounding tissues or spread systemically.

The overall cytocompatibility was further assessed with a direct assay, observing adhesion and proliferation of cells directly cultured onto the patches (Fig. 5).

As shown in Fig. 5 (Fig. 5A, B) both AC16 and Neo-NHDF cells overall adhered to the patches and remained viable throughout the 7-day period. On day 1, both cell types were well dispersed across the patches' surfaces; however, by day 3, PVDF promoted cluster formation (Fig. 5C and D). In contrast, P_PVDF samples facilitated the proper spreading of AC16 cells, enabling the formation of a more uniform monolayer, while also supporting a spread-out morphology in Neo-NHDFs, indicative of good adhesion. For both AC16s and Neo-NHDFs the day 1 and day 3 images show better cell attachment to P_PVDF samples than to PVDF, although by day 7 the AC16 cultures for PVDF and P_PVDF were quite similar.

The differences in relative DNA production between Figs. 4 and 5 will be as a result of (i) changes in the morphology of the material (Fig. 5

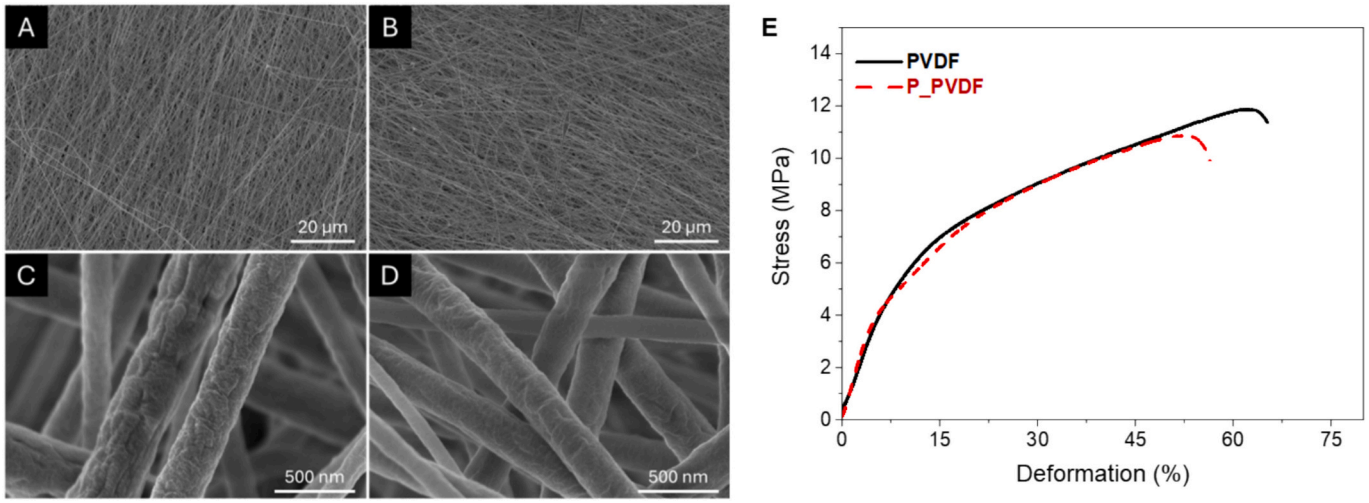

Fig. 3. FESEM images of PVDF (A, C) and P_PVDF (B, D) patches and representative stress-deformation curves (E).

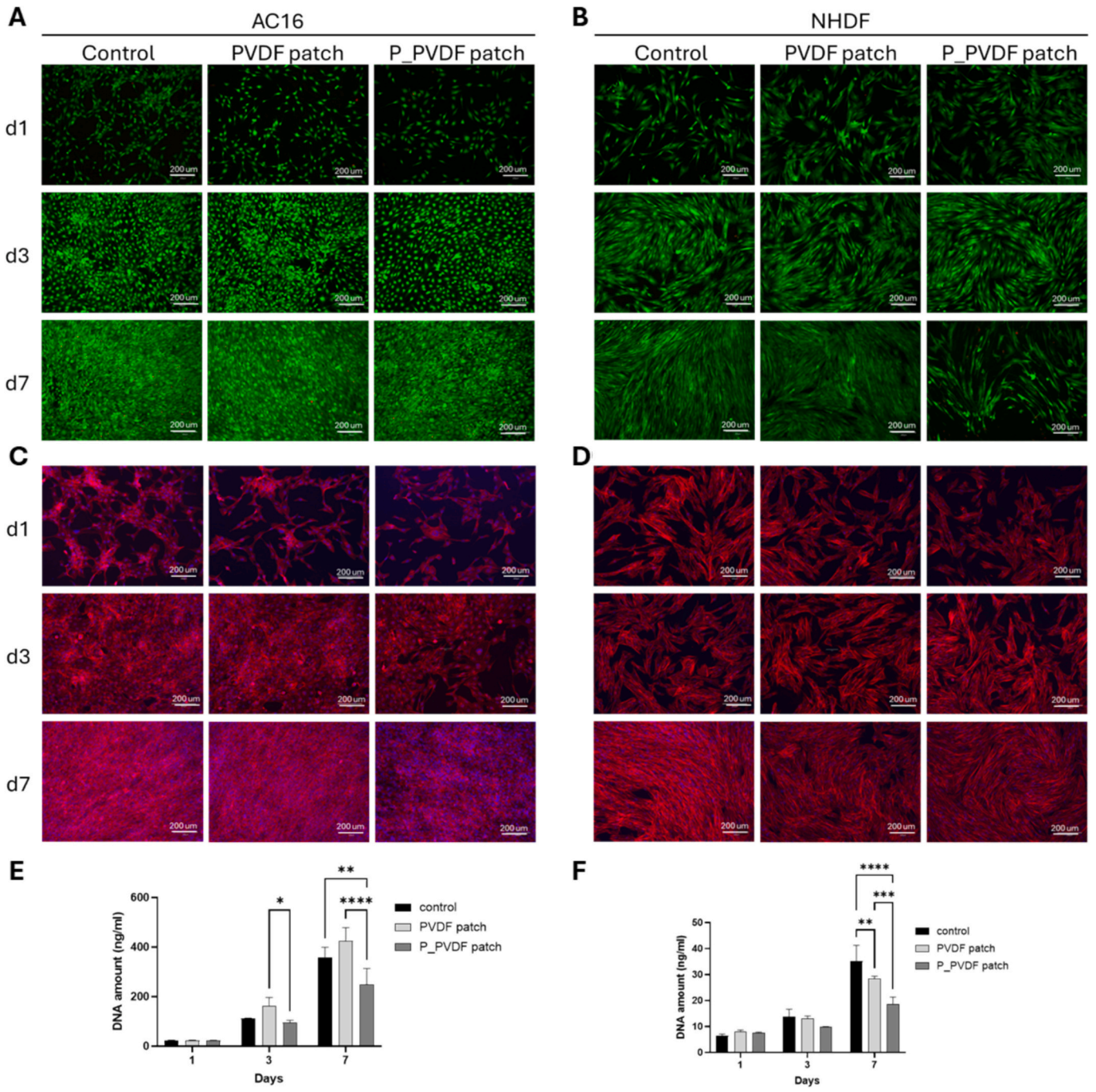

Fig. 4. Indirect assay of PVDF and P_PVDF patches on AC16 and NHDF. Live (green) and dead (red) assay of (A) AC16s and (B) Neo-NHDFs. Immunofluorescence analysis of (C) AC16 and (D) Neo-NHDF, F-actin stained red, nuclei are stained blue. Proliferation assay of (E) AC16 and (F) Neo-NHDF. Scale bars are 200 μm. (For interpretation of the references to colour in this figure legend, the reader is referred to the web version of this article.)

is a complex 3D fibrous architecture whereas Fig. 4 is a 2D culture), and (ii) different rates of cell attachment (in Fig. 4 cells are attaching to tissue culture plastic, a material designed to promote cell attachment). From the standpoint of its intended clinical application, reduced and slower cell proliferation is considered advantageous, as it allows for better exploitation of the patch's piezoelectric properties and its integration with native tissue, while minimizing the risk of uncontrolled tissue overgrowth after implantation [3]. Accordingly, the purpose is not to promote the formation of new tissue around the implant, but rather to support the remodeling of existing tissue through electromechanical coupling. As shown clearly in Fig. 5A and B, the implant material is well tolerated by both cell types. These data further demonstrate that plasma-treated PVDF patches are more effective in supporting cell adhesion and spreading, aligning with studies that have reported enhanced tissue maturation and improved function of primary rat cardiomyocytes when seeded onto similar substrates [3], ultimately supporting their potential use for cardiac tissue regeneration applications.

3.5. *Implantation of PVDF and P_PVDF patches in infarcted mice*

The biocompatibility of the designed patches was further evaluated in a clinically relevant setting by assessing *in vivo* the local inflammatory response to patch implantation and exploring the effectiveness of plasma treatment in enhancing interaction with the host tissue. In detail,

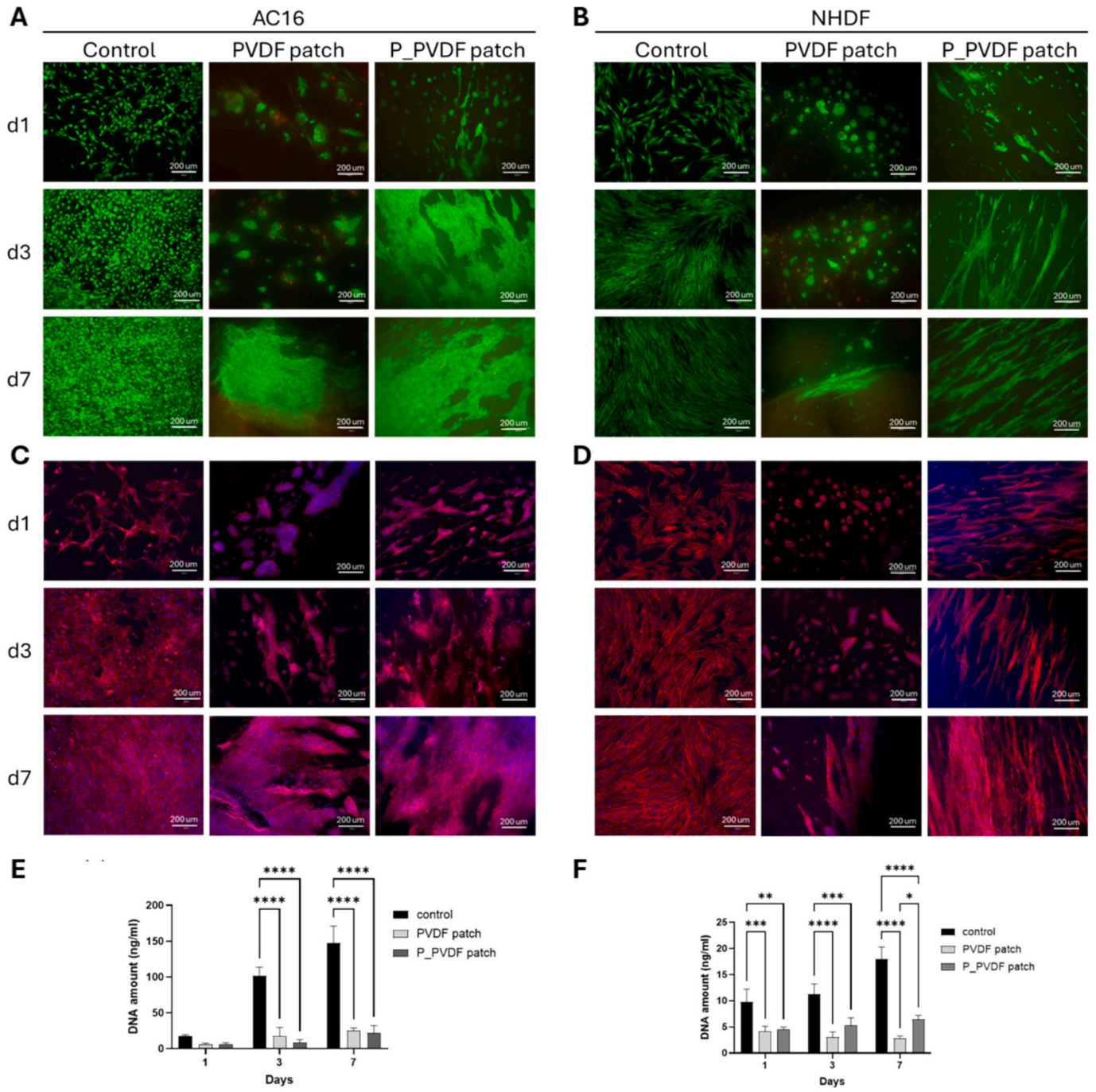

Fig. 5. Direct assay of PVDF and P_PVDF patches on AC16 and NHDF. Live (green) and dead (red) assay of (A) AC16 and (B) Neo-NHDF. Immunofluorescence analysis of (C) AC16 and (D) Neo-NHDF, F-actin stained red, nuclei are stained blue. Proliferation assay of (E) AC16 and (F) Neo-NHDF. Scale bars are 200 μm. (For interpretation of the references to colour in this figure legend, the reader is referred to the web version of this article.)

circular patches with a 4 mm diameter were implanted onto the epicardium of infarcted mice using fibrin glue. The hearts were then harvested after 14 days post-injury (d.p.i.), a timeframe in which the primary acute inflammatory response to MI had subsided (Fig. 6A and Supplementary video 1).

In both groups, PVDF and P_PVDF patches remained securely attached to the epicardium, covering a significant portion of the infarcted left ventricle wall (Fig. 6B). The infarcted area was characterized by extensive collagen deposition and appeared in blue in representative histological sections stained with Masson's Trichrome (Fig. 6C). PVDF patches of both experimental groups remained clearly visible and well-integrated on the ventricular surface, showing no apparent signs of alteration. In addition, no differences were observed between the groups regarding the weight-to-body weight ratio or overall cardiac remodeling following MI (Fig. 6C and D).

Immunofluorescence analysis was performed to evaluate the local infiltration of immune cells ($CD45^+$) around the patch (Fig. 6E). A distinct accumulation of $CD45^+$ cells was observed around non-treated patches, while P_PVDF patches showed a less abundant and more dispersed presence of $CD45^+$ immune cells (Fig. 6E, white arrowheads).

To further quantify these observations while minimizing user-associated bias and variability, a bioinformatic pipeline was developed to automatically detect and quantify $CD45^+$ cells within a defined myocardial area (Fig. S4, Supplementary Information). Compared to

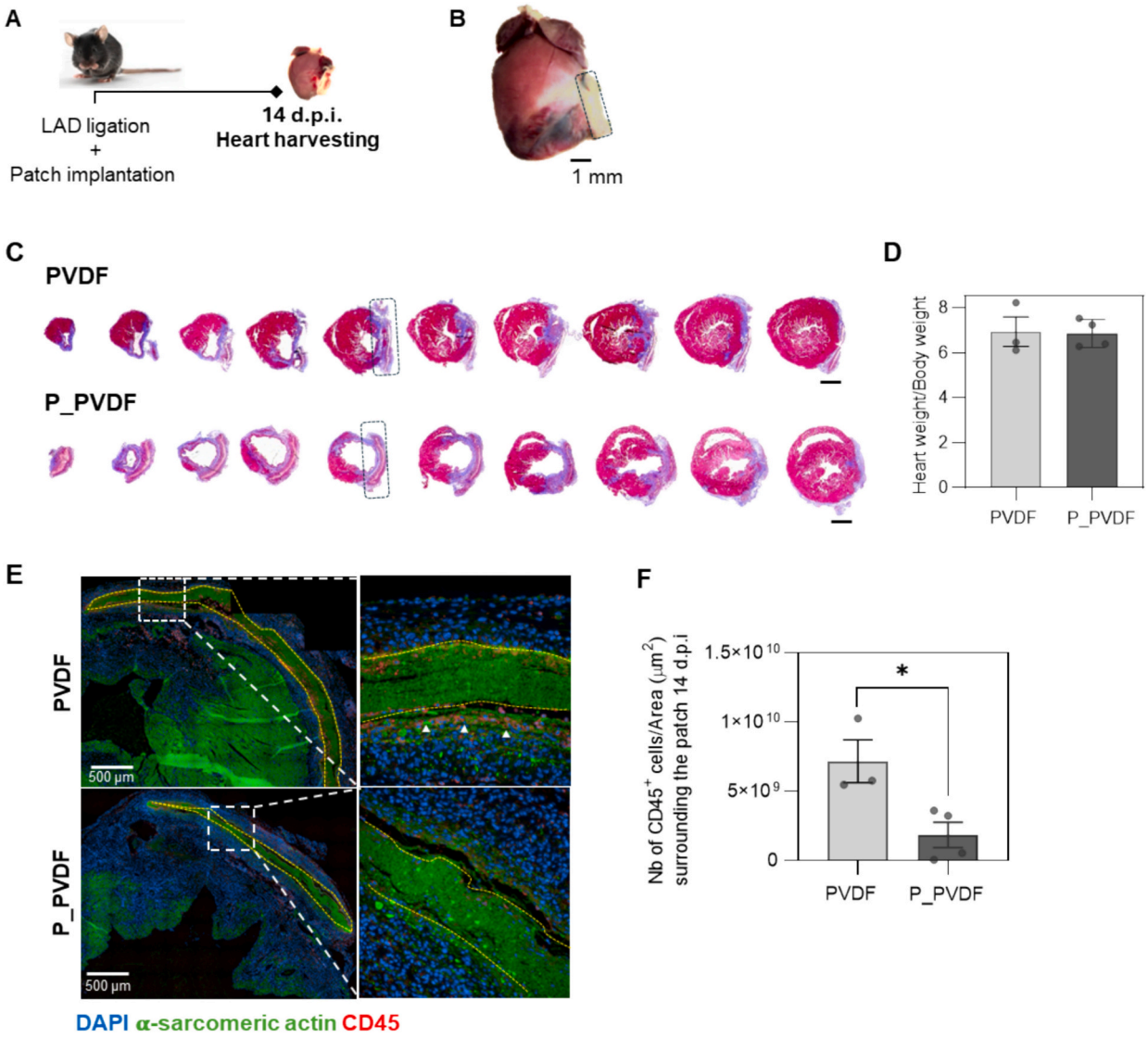

Fig. 6. O_2 plasma surface treatment increases the patch biocompatibility. A) Schematic representation of the experimental setup. B) Representative stereomicroscope image of an infarcted heart showing patch attachment (dashed black line), 14 days post-injury (d.p.i). Scale bar: 1 mm. C) Representative images of the Masson Trichrome staining of transversal sections of the infarcted hearts highlighting the patch region in a dashed box. Scale bar: 1 mm. D) Heart weight/body weight ratio at 14 d.p.i. E) Representative images of the immunofluorescence staining used to detect $CD45^+$ cells, in which the patch is delineated with a dashed yellow line. High magnification insets are present on the left, showing regions of $CD45^+$ cell accumulation (white arrowheads). F) Automated quantification of $CD45^+$ cells around the patch ($n = 3$ animals for PVDF, $n = 4$ animals for P_PVDF patches). Data shown as mean ± SEM, $*p < 0.05$. (For interpretation of the references to colour in this figure legend, the reader is referred to the web version of this article.)

non-treated controls, P_PVDF patches exhibited a significant lower number of immune cells near the patch, indicating that the surface treatment effectively reduced the inflammatory response upon implantation *in vivo* (Fig. 6F). These findings are aligned with evidence demonstrating the superior biocompatibility of plasma-treated patches *in vivo* and *in vitro* in bone and corneal regeneration [31,32]. Regarding the cardiac application of plasma-treated biomaterials, although a limited number of previous studies have demonstrated their biocompatibility in healthy hearts, the lack of quantitative inflammatory assessment and injury-specific patch application has limited direct comparisons with untreated controls in more clinically relevant settings [31]. Here, we have shown that optimized plasma surface treatment significantly enhanced the biological performance of the PVDF patches, ultimately supporting a more functional material-cell interaction *in vivo*. According to the literature, materials with hydrophilic surface properties exhibit greater resistance to immune cell activity and can effectively suppress the secretion of pro-inflammatory cytokines that would otherwise contribute to implant rejection [33,34].

4. Conclusions

PVDF-based biomaterials have shown significant potential for cardiac applications, demonstrating their ability to enhance heart repair following MI in mouse models. However, the hydrophobic nature of PVDF-based devices may pose challenges for integration and clinical application, potentially triggering a prolonged and undesirable immune response. This study demonstrates *in vitro* and *in vivo* that the biocompatibility of electrospun PVDF cardiac patches can be significantly enhanced through optimized radio-frequency low-pressure O_2 plasma treatment.

The methodology employed allowed for a comprehensive investigation of a broad range of parameters, leading to the identification of the most effective and reproducible combination for optimizing the final process. The study revealed that the formation of surface oxygen-

containing hydrophilic groups, and the resulting superhydrophilicity, is promoted by maximizing reactive species for longer treatment times. Conversely, higher plasma power levels compromised the patch's structural and mechanical integrity.

The optimized plasma treatment was confirmed not to alter the patch's mechanical elasticity or fibrous nanostructure, allowing it to mimic the characteristics of native tissue, while also preserving a high content of the electroactive β-phase, which is responsible for the patch's piezoelectricity.

The viability, adhesion, and proliferation of human cardiomyocytes and dermal fibroblasts proved the cytocompatibility of the engineered patches. Accordingly, the O_2 plasma treatment fostered the gradual formation of a cohesive cell layer, in contrast to what observed on the untreated hydrophobic surface. Furthermore, the improvement in the biological performance of the plasma-treated PVDF patches was further demonstrated by its excellent adherence to the epicardium and the marked reduction of immune infiltration following implantation in infarcted mice.

Finally, considering the reported findings and in response to urgent clinical needs, the patch's electroactive and structural characteristics, combined with its favourable elasticity and superhydrophilicity, warrant further exploration for their potential to facilitate effective electromechanical coupling and promote functional cardiac tissue regeneration following acute myocardial infarction.

Supplementary data to this article can be found online at https://doi.org/10.1016/j.bioadv.2025.214488.

CRediT authorship contribution statement

G. Montalbano: Writing – original draft, Visualization, Validation, Methodology, Investigation, Formal analysis, Data curation, Conceptualization. **J. Barberi:** Writing – original draft, Visualization, Validation, Methodology, Investigation, Data curation, Conceptualization. **A. Benedetto Mas:** Writing – original draft, Validation, Methodology, Formal analysis, Data curation. **T. Tung:** Visualization, Validation, Methodology, Formal analysis, Data curation. **P. Melo:** Writing – review & editing, Validation, Methodology, Investigation, Formal analysis, Data curation, Conceptualization. **K. Dalgarno:** Writing – review & editing, Supervision, Resources, Investigation, Conceptualization. **E.D. Silva:** Writing – original draft, Visualization, Validation, Formal analysis, Data curation. **R.N. Gomes:** Visualization, Validation, Methodology, Formal analysis, Data curation. **D.S. Nascimento:** Writing – review & editing, Supervision, Resources, Investigation, Conceptualization. **S. Fiorilli:** Writing – review & editing, Supervision, Resources, Investigation, Conceptualization. **C. Vitale-Brovarone:** Writing – review & editing, Supervision, Resources, Project administration, Funding acquisition, Conceptualization.

Ethics statements

All animal procedures complied with Directive 2010/63/EU of the European Parliament and were approved by the i3S Animal Ethics Committee and the Direcção Geral de Alimentação e Veterinária (permit 022793). Humane endpoints were established following the Organization for Economic Cooperation and Development (OECD) Guidance Document on the Recognition, Assessment, and Use of Clinical Signs as Humane Endpoints for Experimental Animals Used in Safety Evaluation (2000).

Declaration of competing interest

The authors declare that they have no known competing financial interests or personal relationships that could have appeared to influence the work reported in this paper.

Acknowledgments

This project has received funding from the European Union's Horizon Europe research and innovation programme under grant agreement No 101091852 (REBORN). RNG was awarded individual funding through the Fundação para a Ciência e Tecnologia (FCT) [SFRH/BD/144490/2019]. Views and opinions expressed are however those of the author(s) only and do not necessarily reflect those of the European Union or the European Health and Digital Executive Agency (HADEA). Neither the European Union nor the granting authority can be held responsible for them.

The authors would like to acknowledge the BioSciences Screening Unit at i3S and Prof. Stefano Stassi from Politecnico di Torino for his assistance with the measurement of the piezoelectric coefficient of the patches.

Data availability

Data will be made available on request.

References

[1] D. Mangindaan, I. Yared, H. Kurniawan, J. Sheu, e M. Wang, Modulation of biocompatibility on poly(vinylidene fluoride) and polysulfone by oxygen plasma treatment and dopamine coating, J. Biomed. Mater. Res. A 100A, fasc. 11 (2012) 3177–3188, https://doi.org/10.1002/jbm.a.34251.

[2] P.K. Szewczyk, et al., Surface-Potential-Controlled Cell Proliferation and Collagen Mineralization on Electrospun Polyvinylidene Fluoride (PVDF) Fiber Scaffolds for Bone Regeneration, ACS Biomater Sci. Eng. 5, fasc. 2 (2019) 582–593, https://doi.org/10.1021/acsbiomaterials.8b01108.

[3] M. Kitsara, et al., Cyto- and bio-compatibility assessment of plasma-treated polyvinylidene fluoride scaffolds for cardiac tissue engineering, Front. Bioeng. Biotechnol. 10 (2022) 1008436, https://doi.org/10.3389/fbioe.2022.1008436.

[4] M. Kitsara, O. Agbulut, D. Kontziampasis, Y. Chen, e P. Menasché, «Fibers for hearts: A critical review on electrospinning for cardiac tissue engineering», Acta Biomater., vol. 48, pp. 20–40, gen. 2017, doi: https://doi.org/10.1016/j.actbio.2016.11.014.

[5] M. R. Gomes, F. Castelo Ferreira, e P. Sanjuan-Alberte, «Electrospun piezoelectric scaffolds for cardiac tissue engineering», Biomater. Adv., vol. 137, p. 212808, giu. 2022, doi: https://doi.org/10.1016/j.bioadv.2022.212808.

[6] N. Adadi, et al., Electrospun Fibrous PVDF-TrFe Scaffolds for Cardiac Tissue Engineering, Differentiation, and Maturation, Adv. Mater. Technol. 5, fasc. 3 (2020) 1900820, https://doi.org/10.1002/admt.201900820.

[7] B. Azimi *et al.*, «Electrospinning Piezoelectric Fibers for Biocompatible Devices», Adv. Healthc. Mater., vol. 9, fasc. 1, p. 1901287, gen. 2020, doi: https://doi.org/10.1002/adhm.201901287.

[8] L. M. Monteiro *et al.*, «Nanoscale piezoelectric patches preserve electrical integrity of infarcted hearts», Mater. Today Bio, vol. 32, p. 101742, giu. 2025, doi: https://doi.org/10.1016/j.mtbio.2025.101742.

[9] D.M. Correia, et al., Surface wettability modification of poly(vinylidene fluoride) and copolymer films and membranes by plasma treatment, Polymer 169 (2019) 138–147, https://doi.org/10.1016/j.polymer.2019.02.042.

[10] A. Boulares-Pender, I. Thomas, A. Prager, e A. Schulze, Surface modification of polyamide and poly(vinylidene fluoride) membranes, J. Appl. Polym. Sci. 128, fasc. 1 (2013) 322–331, https://doi.org/10.1002/app.38145.

[11] M. Kormunda, P. Ryšánek, P. Hájková, E. Štěpanovská, P. Čapková, e J. Pavlík, Effect of low energy plasma treatment on surface chemistry and phase composition of electrospun polyvinylidene fluoride membrane, Surf Interfaces 22 (2021) 100900, https://doi.org/10.1016/j.surfin.2020.100900.

[12] A. Kaynak, T. Mehmood, X. Dai, K. Magniez, e A. Kouzani, «Study of Radio Frequency Plasma Treatment of PVDF Film Using Ar, O2 and (Ar + O2) Gases for Improved Polypyrrole Adhesion», Materials, vol. 6, fasc. 8, pp. 3482–3493, ago. 2013, doi: https://doi.org/10.3390/ma6083482.

[13] M. D. Duca, C. L. Plosceanu, e T. Pop, «Surface modifications of polyvinylidene fluoride (PVDF) under rf Ar plasma», Polym. Degrad. Stab., vol. 61, fasc. 1, pp. 65–72, gen. 1998, doi: https://doi.org/10.1016/S0141-3910(97)00130-4.

[14] T. Havlíková *et al.*, «Adaptability of Electrospun PVDF Nanofibers in Bone Tissue Engineering», Polymers, vol. 17, fasc. 3, p. 330, gen. 2025, doi: https://doi.org/10.3390/polym17030330.

[15] T. Lei, L. Yu, L. Wang, F. Yang, e D. Sun, «Predicting Polymorphism of Electrospun Polyvinylidene Fluoride Membranes by Their Morphologies», J. Macromol. Sci. Part B, vol. 54, fasc. 1, pp. 91–101, gen. 2015, doi: https://doi.org/10.1080/00222348.2014.983853.

[16] M. Kitsara, et al., Permanently hydrophilic, piezoelectric PVDF nanofibrous scaffolds promoting unaided electromechanical stimulation on osteoblasts, Nanoscale 11, fasc. 18 (2019) 8906–8917, https://doi.org/10.1039/C8NR10384D.

[17] T.L. Laundos, et al., Consistent long-term therapeutic efficacy of human umbilical cord matrix-derived mesenchymal stromal cells after myocardial infarction despite

individual differences and transient engraftment, Front. Cell Dev. Biol. 9 (2021) 624601, https://doi.org/10.3389/fcell.2021.624601.
[18] M. Valente *et al.*, «Optimized heart sampling and systematic evaluation of cardiac therapies in mouse models of ischemic injury: assessment of cardiac remodeling and semi-automated quantification of myocardial infarct size», Curr. Protoc. Mouse Biol., vol. 5, fasc. 4, pp. 359–391, dic. 2015, doi: https://doi.org/10.1002/9780470942390.mo140293.
[19] T. Lei, L. Yu, G. Zheng, L. Wang, D. Wu, e D. Sun, «Electrospinning-induced preferred dipole orientation in PVDF fibers», J. Mater. Sci., vol. 50, fasc. 12, pp. 4342–4347, giu. 2015, doi: https://doi.org/10.1007/s10853-015-8986-0.
[20] Z. He, F. Rault, A. Vishwakarma, E. Mohsenzadeh, e F. Salaün, «High-Aligned PVDF Nanofibers with a High Electroactive Phase Prepared by Systematically Optimizing the Solution Property and Process Parameters of Electrospinning», *Coatings*, vol. 12, fasc. 9, p. 1310, set. 2022, doi: https://doi.org/10.3390/coatings12091310.
[21] X. Cai, T. Lei, D. Sun, e L. Lin, A critical analysis of the α, β and γ phases in poly (vinylidene fluoride) using FTIR, RSC Adv. 7, fasc. 25 (2017) 15382–15389, https://doi.org/10.1039/C7RA01267E.
[22] K. Castkova, et al., Structure–Properties Relationship of Electrospun PVDF Fibers, Nanomaterials 10, fasc. 6, Art. fasc. 6 (2020) giu, https://doi.org/10.3390/nano10061221.
[23] P. J. Gouveia *et al.*, «Flexible nanofilms coated with aligned piezoelectric microfibers preserve the contractility of cardiomyocytes», Biomaterials, vol. 139, pp. 213–228, set. 2017, doi: https://doi.org/10.1016/j.biomaterials.2017.05.048.
[24] A. Vesel *et al.*, «Non-Equilibrium Plasma Methods for Tailoring Surface Properties of Polyvinylidene Fluoride: Review and Challenges», Polymers, vol. 13, fasc. 23, p. 4243, dic. 2021, doi: https://doi.org/10.3390/polym13234243.
[25] N. Vandencasteele, D. Merche, e F. Reniers, XPS and contact angle study of N_2 and O_2 plasma-modified PTFE, PVDF and PVF surfaces, Surf. Interface Anal. 38, fasc. 4 (2006) 526–530, https://doi.org/10.1002/sia.2255.
[26] Y.W. Park, e N. Inagaki, Surface modification of poly(vinylidene fluoride) film by remote Ar, H2, and O2 plasmas, Polymer 44, fasc. 5 (2003) 1569–1575, https://doi.org/10.1016/S0032-3861(02)00872-8.
[27] D. M. Correia *et al.*, «Influence of oxygen plasma treatment parameters on poly (vinylidene fluoride) electrospun fiber mats wettability», Prog. Org. Coat., vol. 85, pp. 151–158, ago. 2015, doi: https://doi.org/10.1016/j.porgcoat.2015.03.019.
[28] M. Kitsara, et al., Permanently hydrophilic, piezoelectric PVDF nanofibrous scaffolds promoting unaided electromechanical stimulation on osteoblasts, Nanoscale 11, fasc. 18 (2019) 8906–8917, https://doi.org/10.1039/C8NR10384D.
[29] G. Zhu, Q. Yuan, J. Hock Yeo, e M. Nakao, Thermal treatment of expanded polytetraflu-oroethylene (ePTFE) membranes for reconstruction of a valved conduit, Biomed. Mater. Eng. 26, fasc. 1_suppl (2015) S55–S62, https://doi.org/10.3233/BME-151289.
[30] A. F. B. A. Fadzil, A. Pramanik, A. K. Basak, C. Prakash, e S. Shankar, «Role of surface quality on biocompatibility of implants - A review», Ann. 3D Print. Med., vol. 8, p. 100082, ott. 2022, doi: https://doi.org/10.1016/j.stlm.2022.100082.
[31] P. Bhattacharjee, P. W. Madden, E. Patriarca, e M. Ahearne, «Optimization and evaluation of oxygen-plasma-modified, aligned, poly (Є-caprolactone) and silk fibroin nanofibrous scaffold for corneal stromal regeneration», Biomater. Biosyst., vol. 12, p. 100083, dic. 2023, doi: https://doi.org/10.1016/j.bbiosy.2023.100083.
[32] D. Kim, et al., Oxygen plasma-modified polycaprolactone nanofiber membrane activates the biological function in cell adhesion, proliferation, and migration through the phosphorylation of FAK and ERK1/2, enhancing bone regeneration, Chem. Eng. J. 499 (2024) 156003, https://doi.org/10.1016/j.cej.2024.156003.
[33] M. Rafiei, J.T. Chung, e Y. Chau, Roles of biomaterials in modulating the innate immune response in ocular therapy, Front. Drug Deliv. 3 (2023) 1077253, https://doi.org/10.3389/fddev.2023.1077253.
[34] K.M. Hotchkiss, G.B. Reddy, S.L. Hyzy, Z. Schwartz, B.D. Boyan, e R. Olivares-Navarrete, Titanium surface characteristics, including topography and wettability, alter macrophage activation, Acta Biomater. 31 (2016) 425–434, https://doi.org/10.1016/j.actbio.2015.12.003.